Detection of a bioluminescent milky sea from space

Steven D. Miller*†, Steven H. D. Haddock‡, Christopher D. Elvidge§, and Thomas F. Lee*

*Marine Meteorology Division, Naval Research Laboratory, 7 Grace Hopper Avenue, MS #2, Monterey, CA 93943; ‡Monterey Bay Aquarium Research Institute, 7700 Sandholdt Road, Moss Landing, CA 95039; and §National Geophysical Data Center, Boulder, CO 80303

Communicated by J. Woodland Hastings, Harvard University, Cambridge, MA, August 19, 2005 (received for review April 29, 2005)

On many occasions over the centuries, mariners have reported witnessing surreal nocturnal displays where the surface of the sea produces an intense, uniform, and sustained glow that extends to the horizon in all directions. Although such emissions cannot be fully reconciled with the known features of any light-emitting organism, these so-called ''milky seas'' are hypothesized to be manifestations of unusually strong bioluminescence produced by colonies of bacteria in association with a microalgal bloom in the surface waters. Because of their ephemeral nature and the paucity of scientific observations, an explanation of milky seas has remained elusive. Here, we report the first satellite observations of the phenomenon. An ≈15,400-km² area of the northwestern Indian Ocean, roughly the size of the state of Connecticut, was observed to glow over 3 consecutive nights, corroborated on the first night by a ship-based account. This unanticipated application of satellite remote-sensing technology provides insights pertaining to the formation and scale of these poorly understood events.

bacterial bioluminescence | satellite remote sensing | microbial ecology | quorum sensing | marine biology

Although reported by mariners since the 17th century (1, 2), milky seas have eluded all but the most rudimentary levels of scientific inquiry, with the exception of a single chance encounter by a research vessel (3). The report from that expedition postulated the light emission to be due to luminous bacteria (*Vibrio harveyi*) living in association with colonies of the microalga *Phaeocystis*. However, details of the formation mechanisms, spatial extent, global distribution, temporal variability, and ecological implications of milky seas remain almost entirely unknown.

The little that is known is derived almost entirely from archived ship logs and is subject to the uncertainties of human perception and predominantly layman interpretation. Based on 235 documented cases reported since 1915, the ''typical'' milky sea (seen only at night) glows continuously over an extensive area, is independent of wind speed, lasts anywhere from several hours to several days, and may be associated with oceanographic fronts or biological slicks (1, 4–6). More than 70% (171) of reported milky seas were encountered in the northwest Indian Ocean, most commonly during the summer southwest monsoon (1), with another, smaller cluster (≈17%) in the waters near Java, Indonesia. Although these statistics are biased toward active shipping routes, reports of milky seas from other heavily trafficked regions are extremely infrequent.

Only two types of luminous organisms are considered to be reasonable candidates for the milky seas emission: dinoflagellates and bacteria. The former, which emit brief (<1 s), bright flashes in response to mechanical disturbance (7), are known to be primarily responsible for the luminescence seen in breaking waves or in the wake of a ship, which may persist for many kilometers in the case of large ships. Given the state of satellite technology and sampling limitations, experts within the remote-sensing community have generally dismissed the prospect of detecting this type of bioluminescence emission from space as unlikely, if not impossible. In any event, it has seemed that there could not be a sustained and uniform stimulation over such large areas, as would be required for dinoflagellates to be the cause of milky seas.

Compared with a dinoflagellate flash (see figure 13 in ref. 3), luminous bacteria emit a continuous but relatively faint (per cell) glow that can persist for many days under appropriate conditions (8, 9). However, the hypothesis that bacteria cause milky seas has been hard to accept because of the demonstrated phenomenon of autoinduction (10, 11), now referred to as quorum sensing (12). The synthesis of the luciferase system in a liquid medium requires a critical concentration of a substance produced by the cells themselves, and the cell density required to achieve this level is quite high, $\approx 10^8$ cells·ml^{-1} (10). Indeed, it has been shown that free-living planktonic luminous bacteria in the ocean typically do not emit light, even though they are luminous when cultured.¶ However, if cells are growing on a solid substrate (for example, as colonies on a solid medium), induction can occur in very small colonies, because concentrations of autoinducer are locally high (14). The postulated association of luminous bacteria with colonies of *Phaeocystis* (3) would provide such conditions, leading to autoinduction, so that the population of luminous bacteria would emit continuously at a rate of perhaps 10^3 photons·s^{-1}·cell^{-1} (15).

The inherent difficulty of collecting observations over the world's oceans makes the task of learning more about the milky seas phenomenon well suited to remote sensing from satellites. This study reports the first detection by satellite sensors of a milky sea event, located in the northwest Indian Ocean.

Materials and Methods

Satellite Sensor. This study used measurements from the U.S. Defense Meteorological Satellite Program constellation of satellites. These 833-km altitude, polar-orbiting satellites feature the Operational Linescan System (OLS), which is designed to monitor global cloudiness under both solar and lunar illumination. For nighttime observations, the OLS utilizes a photomultiplier tube (PMT) with a gallium arsenide opaque photocathode to collect visible/near infrared (VNIR) light (over the wavelength range 470–950 nm) at a sensitivity that is roughly four orders of magnitude higher than conventional visible-band silicon detectors such as those on the Advanced Very High Resolution Radiometer and Landsat Thematic Mapper (16). The earth scene is imaged by means of an oscillating scanning pattern normal to the satellite ground track. A constant sample rate and mechanical reduction of the PMT electron aperture for the outer quarter of each scan line result in roughly equal pixel area (≈2.8 km) across its 3,000-km swath width. Although the VNIR nighttime band provides superb contrast information across a wide dynamic range, it is limited by coarse radiometric resolution (8-bit quantization) and lacks calibration. In addition to lunar reflection sensing, its low-light imaging capability has been used to detect terrestrial and atmospheric emission sources such as fires, lightning, and human activity (e.g., city lights and fishing boats employing floodlights) around the world (16–18).

Abbreviations: OLS, Operational Linescan System; VNIR, visible/near infrared; GMT, Greenwich Mean Time.

†To whom correspondence should be addressed. E-mail: miller@nrlmry.navy.mil.

¶Booth, C. K. & Nealson, K. H. (1975) *Biophys. J.* **15,** 56 (abstr.).

There are no previous reports on capabilities of the OLS to detect milky seas or any other bioluminescence.

Digital Enhancement of Satellite Imagery. To improve the visual contrast between the coherent milky sea emission structure and instrument background noise, the OLS-VNIR data were digitally enhanced. First, the mean intensity of each scan line was subtracted to reduce any noise-floor variations (e.g., striping artifacts). To reduce photomultiplier tube noise, a 3-pixel (≈8 km) filter was then applied in the scan-line direction. If at least 2 pixels exceeded a threshold (set at ≈5% of detector saturation), then all 3 pixels were set to the saturation value (63 digital counts); otherwise, all 3 pixels were set to zero. This procedure was repeated in the along-track direction. Finally, an 8-pixel (≈20 km) boxcar filter was applied, and the data were histogram-equalized. The enhancement results in the gathering of coherent features and suppression of random noise.

Bacterial Culture and Spectra. Emission spectra reported for several different species of luminous bacteria give peak values at ≈490 nm and half-bandwidths of ≈70 nm (19, 20). *Vibrio fischeri* strains (Carolina Biological Supply), whose emission spectra are representative of the luminous bacteria species thought to be responsible for milky seas (e.g., *V. harveyi*), were grown in *Photobacterium* broth (Carolina Biological Supply). Bacterial emission spectra were measured with a monochromator (Princeton Instruments, Trenton, NJ) coupled to a back-illuminated charge-coupled device spectrometer. The spectra were required for determination of the detection threshold bacterial radiance, as described below.

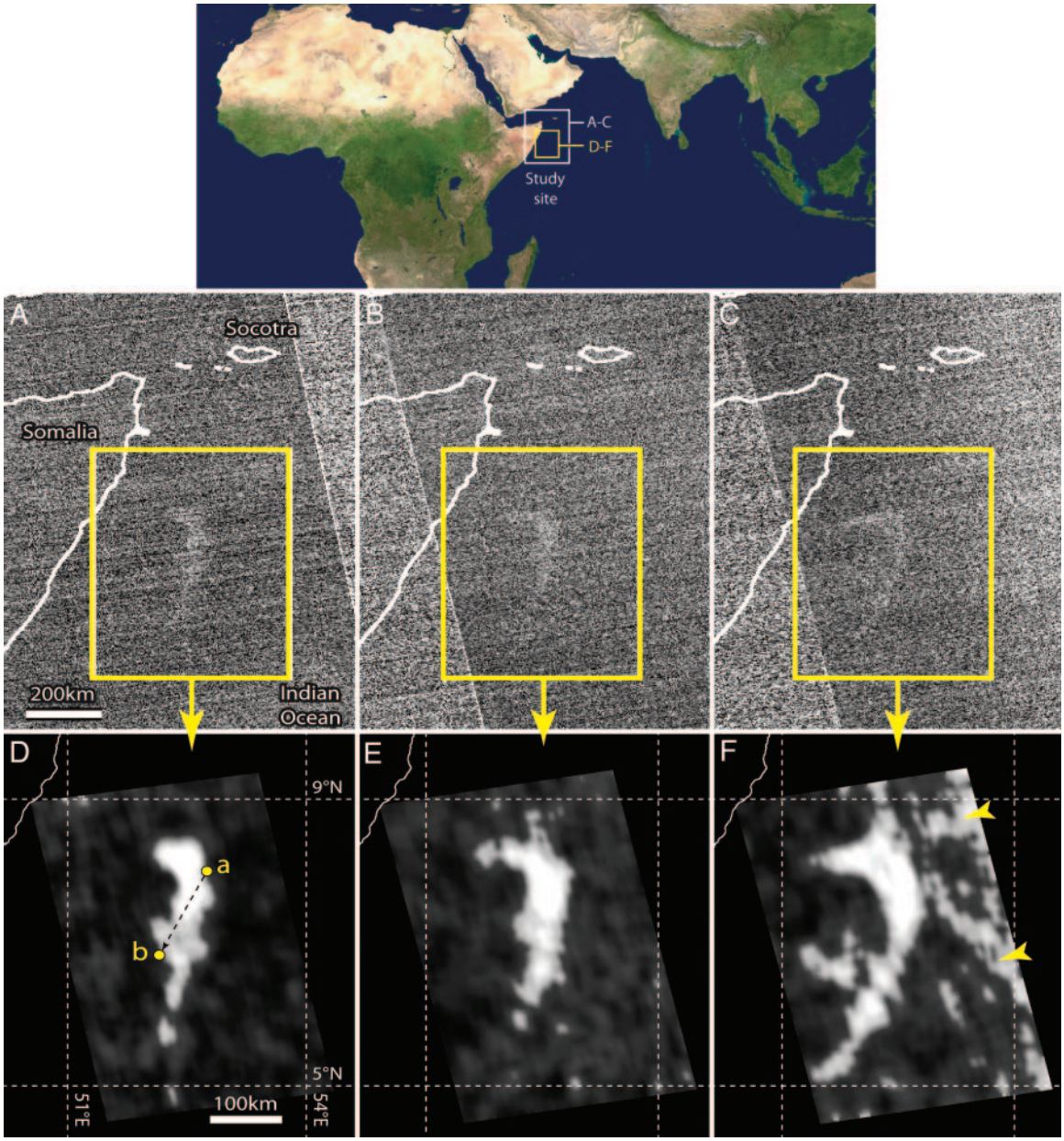

Fig. 1. Study areas (*Top*) corresponding to unfiltered (*A–C*) and filtered (*D–F*) satellite imagery on the night of the SS *Lima* observations. (*A* and *D*) Jan. 25, 1995, 1836 GMT. (*B* and *E*) Jan. 26, 1995, 1804 GMT. (*C* and *F*) Jan. 27, 1995, 1725 GMT. Arrowheads in *F* indicate low signal-to-noise ratio artifacts. Shown in *D* are the ship track (dashed line) and positions at time of first sighting on the horizon (point a) and exit from the glowing waters (point b), based on details of the ship report.

Sensitivity of Satellite Detectors to Bacterial Emission Spectra. The satellite device measures the scene radiance integrated across the spectral bandwidth of the detector, weighted by the sensor response function. Because the bacterial spectrum does not completely overlap this response function, only a fraction of the total emitted light will be detected, which means that bacteria must produce more light than the nominal minimum detectable signal (MDS) of the instrument to be detected. The fraction (F) of a normalized bacterial emission spectra (B_λ) detected by a satellite sensor characterized by spectral response function (ϕ_λ), given atmospheric transmittance [T_λ, based here on moderate-resolution radiative transfer (MODTRAN) (21) calculations with moisture/haze conditions representative of the sample region], was specified according to the following convolution:

$$F = \int_{\lambda=0}^{\infty} B_\lambda T_\lambda(\theta)\phi_\lambda d\lambda \Big/ \int_{\lambda=0}^{\infty} \phi_\lambda d\lambda, \qquad [1]$$

where θ is the satellite zenith angle defining the path traveled by the radiation through the atmospheric column. Dividing the nominal MDS by F yields the sensor-specific threshold bacterial radiance ($L_{\min}$) for satellite detection.

Bacterial Population Estimates. For a near-surface emitting layer (in-water scattering and absorption neglected) and assumed per-cell photon production rate (P_{bac}; isotropic), the minimum bacterial population ($C_{\min}$, in cells·m^{-2}) required to produce the threshold OLS scene radiance (from Eq. **1**) is obtained by converting $L_{\min}$ to an equivalent flux of photons and dividing by the upwelling hemisphere contribution of P_{bac}:

$$C_{\min} = \pi L_{\min} \frac{\lambda}{hc} \frac{2}{P_{\text{bac}}}. \qquad [2]$$

The scalar product between the satellite-detected area of the milky sea (A_{ms}) and $C_{\min}$ then provides a conservative estimate (assuming that only the minimum detectable radiance was attained) of the total bacterial cell population (C_{tot}).

Results and Discussion

Remote detection of a relatively weak light signal such as bioluminescence depends on its spatial extent, homogeneity, and the effects of atmospheric attenuation and requires the absence of light contamination from other sources. We searched ship reports of milky sea sightings since 1992 (provided by P. J. Herring, personal communication), corresponding to the availability of archived OLS satellite data, for those most likely to be detectable. Of 11 promising events reported, only 1 met all detection criteria: an account from the British merchant vessel SS *Lima* while transiting the northwestern Indian Ocean (22):

> "25 January 1995. At 1800 [GMT] (2100 local time) on a clear moonless night while 150 [nautical] mile[s] east of the Somalian coast, a whitish glow was observed on the horizon and, after 15 minutes of steaming, the ship was completely surrounded by a sea of milky-white color with a fairly uniform luminescence. The bioluminescence appeared to cover the entire sea area, from horizon to horizon . . . and it appeared as though the ship was sailing over a field of snow or gliding over the clouds. . . . The bow waves and the wake appeared blackish in color, and thick black patches of oil were passing by. Later, the Aldis lamp revealed that the 'oil patches' were actually light green kelp, amazingly black against the white water."

Unprocessed OLS nighttime visible imagery from approximately one-half hour into this encounter indicates the presence of a large, bright feature near the *Lima*'s location, which was observed to persist over the next 2 nights (Fig. 1 *A–C*). Digital enhancement and filtering of the imagery (Fig. 1 *D–F*) further separates the coherent feature from the background noise. Positions of the *Lima* reported over the course of its encounter (annotations a and b in Fig. 1*D*) coincide closely with the boundaries of the satellite-observed bright anomaly. The ship recorded its initial coordinates (08.02° N, 52.76° E) when a glow was first noted on the horizon (point a). Knowledge of the *Lima*'s heading and speed allowed for extrapolation to the point at which the crew reported leaving the feature after 6 h (146 km) of steaming (point b).

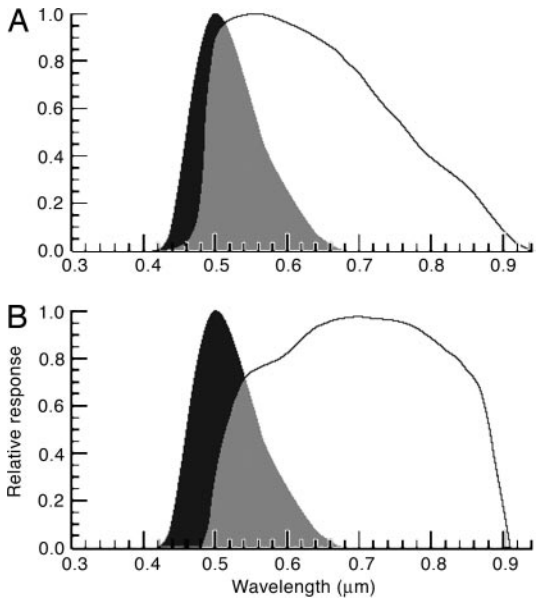

Fig. 2. Laboratory emission spectra of bioluminescent bacteria (black area) compared with spectral response functions. Data are shown for the U.S. Defense Meteorological Satellite Program OLS nighttime visible band of the sensor used in this study (*A*) and the proposed National Polar-orbiting Operational Environmental Satellite System Visible/Infrared Imager/Radiometer Suite day/night band (*B*). Regions of spectral overlap are shown in gray.

The satellite perspective reveals the structure of this truly massive event, spanning an area of at least 15,400 km^2 on Jan. 25, 1995, and expanding to >17,700 km^2 the next day. Persistence of the feature over several days is consistent with previous findings (1, 3) and allows for the examination of its spatial evolution in relation to local sea surface currents. The Navy Layered Ocean Model (23) revealed the presence of a cold-core eddy (24) centered on the northern portion of the emission feature, explaining in part its observed counterclockwise rotation (see Fig. 1 *D–F*) over the 3-day period and the *Lima*'s observation of kelp (more common to coastal regions) almost 280 km offshore. Such accumulation zones are known to be preferred habitats for phytoplankton colonies, wherein a bloom could provide a substrate for the colonization of luminous bacteria (14, 25).

To assess the emission requirements for satellite detection of this milky sea under the assumptions of a bacterial source, we compared the spectral sensitivity of the satellite sensor to the bacterial emission spectrum. Accounting for the solid angle [in steradians (sr)] subtended by the VNIR detector, the in-band minimum detectable signal scene radiance is 4×10^{-5} W·m^{-2}·sr^{-1} (for a signal-to-noise ratio of 6). However, the spectral sensitivity of the VNIR does not completely overlap the bacterial emission spectrum (Fig. 2*A*), so that only a fraction of the total energy emitted by the bacteria would in fact be

ENVIRONMENTAL SCIENCES

detectable. This detection efficiency (22% for the OLS) was calculated by using Eq. **1** to yield an adjusted detection threshold radiance for bacterial emissions of 1.8×10^{-4} W·m^{-2}·sr^{-1} (or 1.4×10^{11} photons·cm^{-2}·s^{-1}).

Using Eq. **2** and assuming a 10^3 photons·s^{-1}·cell^{-1} production rate (15) for fully induced bacteria occurring as a thin layer near the surface, we estimate the minimum water-column-integrated population required for OLS detection to be 2.8×10^8 cells·cm^{-2} (compared with 6×10^8 cells·cm^{-2} measured in ref. 3, which was based on a phytoplankton aggregate from a plankton tow). Based on the satellite-estimated area coverage, the corresponding total population (C_{tot}) of this milky sea was estimated to be $\approx 4 \times 10^{22}$ bacteria cells. Given the many uncertainties in the assumptions and measurements, these numbers should be regarded as approximate.

The next generation of low-light sensors, represented by the day/night band (DNB; e.g., ref. 26) on the National Polar-orbiting Operational Environmental Satellite System (NPOESS) Visible/Infrared Imager/Radiometer Suite (VIIRS), offers the possibility of improved low-light observation capabilities through improved dynamic range, higher signal-to-noise ratio, calibrated data, higher radiometric resolution, superior temporal sampling, and complementary spectral information from other geospatially matched VIIRS channels However, the DNB does not include a requirement for the detection of bioluminescence, and its current design calls for reduced short-wavelength sensitivity in comparison to the OLS-VNIR. This departure would make it less suited for measuring the blue-green bioluminescence emissions produced by bacteria (Fig. 2*B*). Applying Eq. **1** to the proposed DNB spectral response function and detector sensitivity (resulting in an 11% bacterial emission detection efficiency), the detection threshold radiance was estimated at 3.5×10^{-4} W·m^{-2}·sr^{-1} (2.8×10^{11} photons·cm^{-2}·s^{-1}), or about half as sensitive as the current OLS-VNIR. Given the demonstrated ability to detect a unique biological phenomenon, and considering the apparent proximity of these signals to the sensor minimum detectable signal, it may be worth maintaining this shorter wavelength spectral response to optimize detection in the NPOESS era.

A rare opportunity to match satellite low-light sensor observations to surface reports has yielded the first satellite measurements of bioluminescence from a milky sea. The observed translation and rotation of the bright structure over 3 nights was consistent with a cold-core eddy analyzed from an ocean currents model. Satellite remote sensing represents the only viable means of targeting this elusive class of marine bioluminescence. For example, emerging daytime satellite-based techniques for assessing phytoplankton physiology (13) could assist in prioritizing search regions, and confirmation by nighttime sensors of active milky sea events would allow then for their targeting by well equipped research vessels. Combined with remote observations, the *in situ* data collected by these cruises would help us to better understand the role, behavior, and environmental implications of milky seas, shedding light on a long-standing mystery of maritime lore.

We thank Ole Martin Smedstad and Jan Dastugue for contributing Navy Layered Ocean Model analyses, Denis Klimov for radiometric assistance, Lynne Christianson for laboratory help, James Case and Peter Herring for enlightening discussions, and Linda Norton for assistance in literature review. Natural color land data were provided by the National Aeronautics and Space Administration Earth Observatory's MODerate-resolution Imaging Spectroradiometer (MODIS) Blue Marble Project. This work was supported by Office of Naval Research Grant PE-062435N and the David and Lucile Packard Foundation.

1. Herring, P. J. & Watson, M. (1993) *Mar. Obs.* **63,** 22–30.
2. Buist, G. (1855) *Proc. Bombay Geogr. Soc.* 108–125.
3. Lapota, D., Galt, C., Losee, J. R., Huddell, H. D., Orzech, J. K. & Nealson, K. H. (1988) *J. Exp. Mar. Biol. Ecol.* **119,** 55–81.
4. Turner, R. J. (1965) *Notes on the Nature and Occurrence of Marine Bioluminescent Phenomena, Internal Report No. B4* (National Institute of Oceanography, Wormley, U.K.).
5. Staples, R. F. (1966) *The Distribution and Characteristics of Surface Bioluminescence in the Oceans, Technical Report TR-184* (U.S. Naval Oceanographic Office, Washington, DC).
6. Kelly, M. G. & Tett, P. (1978) in *Bioluminescence in Action*, ed. Herring, P. J. (Academic, London), pp. 399–417.
7. Krasnow, R., Dunlap, J., Taylor, W., Hastings, J. W., Vetterling, W. & Gooch, V. D. (1980) *J. Comp. Physiol.* **138,** 19–26.
8. Hastings, J. W. & Nealson, K. H. (1977) *Annu. Rev. Microbiol.* **31,** 549–595.
9. Nealson, K. H. & Hastings, J. W. (1979) *Microbiol. Rev.* **43,** 496–518.
10. Nealson, K. N., Platt, T. & Hastings, J. W. (1970) *J. Bacteriol.* **104,** 313–322.
11. Rosson, R. A. & Nealson, K. N. (1981) *Arch. Microbiol.* **129,** 299–304.
12. Fuqua, W. C., Winans, S. C. & Greenberg, E. P. (1994) *J. Bacteriol.* **176,** 269–275.
13. Behrenfeld, M. J., Boss, E., Siegel, D. A. & Shea D. M. (2005) *Global Biogeochem. Cycles* **19,** GB1006.
14. Barak, M. & Ulitzur, S. (1981) *Curr. Microbiol.* **4,** 597–601.
15. Hastings, J. W. (1978) in *Methods in Enzymology*, ed. DeLuca, M. (Academic, New York), Vol. 57, pp. 125–135.
16. Elvidge, C. D., Baugh, K. E., Kihn, E. A., Kroehl, H. W. & Davis, E. R. (1997) *Photogrammetric Eng. Remote Sens.* **63,** 727–734.
17. Croft, T. A. (1978) *Sci. Am.* **239,** 68–79.
18. Elvidge, C. D., Baugh, K. E., Dietz, J. B., Bland, T., Sutton, P. C. & Kroehl, H. W. (1999) *Remote Sens. Environ.* **68,** 77–88.
19. Hastings, J. W. & Morin, J. G. (1991) in *Neural and Integrative Animal Physiology*, ed. Prosser, C. L. (Wiley Interscience, New York), pp. 131–170.
20. Seliger, H. H. & Morton, R. A. (1968) in *Photophysiology*, ed. Giese, A. C. (Academic, New York), Vol. 4, pp. 253–314.
21. Berk, A., Bernstein, L. W. & Robertson, D. C. (1983) MODTRAN (Philips Laboratory, Report AFGL-TR-83-0187, Hanscom Air Force Base, MA).
22. Briand, J. P. (1996) *Mar. Obs.* **66,** 12–13.
23. Smedstad, O. M., Hurlburt, H. E., Metzger, E. J., Rhodes, R. C., Shriver, J. F., Wallcraft, A. J. & Kara, A. B. (2003) *J. Mar. Syst.* **40–41**, 341–361.
24. Tang, D. L., Kawamura, H. & Luis, A. J. (2002) *Remote Sens. Environ.* **81,** 81–89.
25. Nealson, K. & Hastings, J. W. (1991) in *The Prokaryotes*, eds. Balows, A., Trüper, H. G., Dworkin, M., Harder, W. & Schleifer, K. H. (Springer, New York), 2nd Ed., Vol. 1, Part 2, pp. 625–639.
26. Lee, T. F., Miller, S. D., Schueler, C. F., Hawkins, J. D., Turk, F. J., Richardson, K. & Kent, J. (2004) *Proc. SPIE* **5658,** 1–10.